THE JOURNAL OF PHYSICAL CHEMISTRY B

Article

pubs.acs.org/JPCB

Synergistic Rate Boosting of Collagen Fibrillogenesis in Heterogeneous Mixtures of Crowding Agents

Jean-Yves Dewavrin,[†,‡,§] Muhammed Abdurrahiem,[†,‡] Anna Blocki,[∥] Mrinal Musib,[†] Francesco Piazza,*[,⊥] and Michael Raghunath*[,†,‡,#]

[†]Department of Biomedical Engineering, Faculty of Engineering, National University of Singapore, 117510 Singapore

[‡]NUS Tissue Engineering Programme, Life Sciences Institute, National University of Singapore, 117510 Singapore

[§]NUS Graduate School for Integrative Sciences and Engineering: Centre for Life Sciences, #05-01, 28 Medical Drive, 117456 Singapore

[∥]Singapore Bioimaging Consortium, A*STAR, 138667 Singapore

[⊥]Université d'Orléans and Centre de Biophysique Moléculaire, rue Charles Sadron, F-45071, Orléans, France

[#]Department of Biochemistry, Yong Loo Lin School of Medicine, National University of Singapore, 117599 Singapore

Supporting Information

ABSTRACT: The competition for access to space that arises between macromolecules is the basis of the macromolecular crowding phenomenon, known to modulate biochemical reactions in subtle ways. Crowding is a highly conserved physiological condition in and around cells in metazoans, and originates from a mixture of heterogeneous biomolecules. Here, using collagen fibrillogenesis as an experimental test platform and ideas from the theory of nonideal solutions, we show that an entropy-based synergy is created by a mixture of two different populations of artificial crowders, providing small crowders with extra volume occupancy when in the vicinity of bigger crowders. We present the physiological mechanism by which synergistic effects maximize volume exclusion with the minimum amount of heterogeneous crowders, demonstrating how the evolutionarily optimized crowded conditions found *in vivo* can be reproduced effectively *in vitro*.

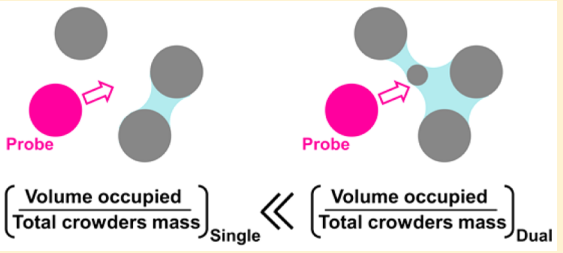

INTRODUCTION

Physiological microenvironments contain high concentrations of macromolecules, up to 400 mg·mL^{-1} in bacterial cytoplasm[1] or 350 mg·mL^{-1} in human blood.[2] At such concentrations, voluminous macromolecules compete for space, transforming the thermodynamic landscape of the crowded solution[2,3] and slowing down macromolecular diffusion.[4] Biological reactions *in vivo* are hence not only characterized by the molecules involved but also by the limited space in which these molecules diffuse. The mechanisms by which excluded-volume effects (EVE) modulate biochemical processes are becoming a growing focus in cell biology, as crowding was revealed to be a major driver of DNA replication,[5] gene expression,[6] compaction[7] and supercoiling of DNA,[8] enzymatic reactions,[9] protein aggregation,[10] folding,[3,11] stability,[11a] and polymerization,[12] along with extracellular matrix deposition by cells.[13] Well-defined *in vitro* crowded conditions also proved beneficial for RT-PCR.[1] In all cases, the boost of biochemical reactions results from an increase of the effective concentration of reactants due to the *excluded volume effect*.[14] Other effects of crowding, such as spatial confinement and depletion forces,[15] can also affect specific stages of biochemical reactions by stabilizing the interaction between two reactants.

The volume excluded by crowders is generally expressed as the volume of crowder molecules themselves. Here we demonstrate that our current crowding efficiencies, yielded by homogeneous crowding, are far below their natural optimum. We also present a detailed solution to overcome this drawback. Physiological microenvironments are crowded with heterogeneous populations of crowders, and the advantages of mixed crowding over homogeneous crowding have been suggested experimentally by other research groups.[16] Zhou tested the effects of mixed crowding on protein stability and suggested that optimal crowding effects could be obtained by adjusting mixing ratios between populations.[16a] In addition, in a recent *in silico* study at lower than physiological temperatures (27 °C), Shah et al. suggested a role for enthalpic interactions in mixtures.[17] However, the underlying *in vitro* mechanism at physiological temperatures (37 °C) was not fully addressed by this study, and remains unclear.

Here, we describe this mechanism. We show that mixing crowders of different sizes generates a synergistic effect, as small crowders bring about extra volume occupancy when in the

Received: August 1, 2014
Revised: February 24, 2015

DOI: 10.1021/jp5077559
J. Phys. Chem. B XXXX, XXX, XXX−XXX

vicinity of bigger crowders, beyond the volume occupied by their structure. As a test platform, we used the kinetics of collagen nucleation and fiber growth, which are driven by diffusion-limited aggregation[18] and can be assessed macroscopically by spectrophotometry.[19] We also tested a wide range of crowders including polyvinylpyrrolidone[20] (PVP), dextran,[7] and Ficoll.[3,10,13]

MATERIALS AND METHODS

1. Collagen Turbidimetry Assays in Crowded Conditions. Bovine dermis collagen I (3.2 mg·mL^{-1} in acetic acid, Koken IAC-30, Japan) was diluted to a 1× PBS, pH 7.4, 1.6 mg·mL^{-1} collagen I solution using 0.05 M acetic acid, 10× PBS (1st Base, Singapore), and 0.15 M NaOH. This solution was finally diluted at 1:1 with plain PBS, or PBS containing macromolecular crowders. The crowders used were PVP 40 kDa and 360 kDa, dextran 70 kDa and 200 kDa (Sigma-Aldrich, Saint Louis, MO), along with Ficoll 70 kDa and 400 kDa (GE Healthcare, Fairfield, CT). Final solutions had a collagen I concentration of 0.8 mg·mL^{-1}. All preparation steps were performed on ice. Immediately after preparation, collagen solutions were transferred to a 37 °C prewarmed 96-well plate (100 μL per well) (UV-Star microplates, F-bottom, Greiner Bio-One GmbH, Frickenhausen, Germany). Absorbance at 313 nm was measured every 20 to 30 s with a Tecan Infinite M200 spectrophotometer (Maennedorf, Switzerland).

2. Calculation of Mixed Crowding Theoretical Effects. We chose collagen nucleation lag time as a readout, as this parameter allowed us to extract a simple measure of *specific* lag time reduction via simple linear fits. Indeed, as it is clearly illustrated by Figure S2 (Supporting Information), the predicted decrease given by eqs 9 and 10 is virtually indistinguishable from a simple linear decrease. This turned out to be true for all types of crowders considered (Figure S3, Supporting Information). As a consequence, we fitted straight lines to all experimental relative lag times (Figure S2, Supporting Information), the slope of which yielded the *specific* effect of each crowder, i.e., lag-time reduction per milligram.

For instance, we measured that each milligram of the crowder dextran 70 kDa decreases the relative nucleation lag time by 0.041. By comparison, each milligram of dextran 200 kDa decreases the relative nucleation lag time by 0.04. According to our *null hypothesis*, which neglects the presence of the void volume, crowding effects are purely additive in a mixture. A mixture of 5 mg·mL^{-1} dextran 70 and 5 mg·mL^{-1} dextran 200 should therefore yield a relative lag time given by eq 1:

$$1 - (5 \times 0.041 + 5 \times 0.04) = 0.595 \tag{1}$$

In order to avoid additional interactions between the two populations of crowders, we used mixtures of two populations sharing the same structure but differing by their molecular weight: (Ficoll 70:Ficoll 400), (dextran 70:dextran 200), and (PVP 40:PVP 360). Theoretical lag times were calculated via this method for a range of mixture ratios, and compared with experimental measurements.

Statistical Analysis. t tests were performed on compared populations of $n = 4$ (two samples of equal variance, two-tailed distribution). A statistical significance between two populations is represented by * ($P > 0.95$).

3. Hard Particle Modeling from a Colloid Physics Perspective. It is reasonable to assume that the measured nucleation rates of collagen triple helices are proportional to the rate of diffusive encounters between collagen monomers. Accordingly, the growth rate should be proportional to the encounter rate of collagen monomers (or oligomers) with larger forming aggregates. Bimolecular encounters in a dilute fluid of hard convex bodies are well described by the Smoluchowski theory,[21] which maps an N-body problem onto an effective two-body problem. Under the hypothesis that the polymerization reaction proceeds much faster than diffusive encounters, the encounter rate can be computed as the stationary flux of a diffusive current J into a sink of radius σ (the diameter of one monomer) and corresponding to a bulk density ρ_B. The solution of this problem is the well-known Smoluchowski rate k_S, given by

$$k_S = -\int_{S_\sigma} \vec{J}\cdot\hat{n}\, dS = 8\pi D_0 \sigma \rho_B \tag{2}$$

Here, $\vec{J} = -2D_0\nabla\rho$ is the stationary particle current, with D_0 being the collagen monomer bare diffusion coefficient, and S_σ is the encounter sphere of radius σ (with the normal vector pointing outward). It should be noted that the bare diffusion coefficient D_0 does not vary appreciably in our study, as (absolute) temperature and viscosity changes are negligible. As we shall see, crowding effects can however be rationalized in terms of an increase in the *collective* diffusion coefficient caused by the crowding-induced excess (with respect to the ideal case) osmotic pressure of the collagen fluid.

A Simple Estimate for the EVE-Induced Increase of the Rate. Equation 2 already provides a first clue as to why the polymerization rate increases with the density of crowders. In fact, the effect of the latter is to reduce the volume available to collagen monomers, thus effectively raising their bulk density. This can be made more quantitative by an *effective-medium* argument analogous to the idea leading to the van der Waals equation. If we imagine the mixture to be composed of N_c collagen monomers (each occupying a volume v_c) and N_s crowding agents (each occupying a volume v_s) in the volume V, the effective volume fractions of the two species will be given by

$$\phi_\alpha = \frac{N_\alpha v_\alpha}{V - N_\beta v_\beta} = \frac{\phi_\alpha(0)}{1 - \phi_\beta(0)} \tag{3}$$

where $\alpha \neq \beta$ = c, s. The above equations can be solved for the effective volume fractions ϕ_c (ϕ_s) and ϕ_s (ϕ_c), leading to

$$\phi_\alpha(\phi_\beta) = \frac{\phi_\alpha(0)}{1 - \phi_\beta(1 - \phi_\alpha(0))} \tag{4}$$

As a consequence, recalling eq 2, the enhancement of collagen−collagen encounter rate due to purely excluded-volume effects arising from the presence of crowders can be estimated as

$$\frac{k_S(\phi_s)}{k_S(0)} = \frac{1}{1 - \phi_s(1 - \phi_c(0))} \tag{5}$$

Local-Density Theory of Bimolecular Encounters in Nonideal Solutions. One of us has shown earlier how the crowding-induced enhancement of bimolecular encounters can be rationalized for the Smoluchowski problem at high densities in terms of an increase of the osmotic pressure that also increases the particle current into the sink.[22] These arguments have been further developed and made more rigorous in terms of a local-density approximation (LDA).[23] In particular, it has been shown that the encounter in a nonideal fluid can be linked

DOI: 10.1021/jp5077559
J. Phys. Chem. B XXXX, XXX, XXX−XXX

to the excess chemical potential (with respect to the ideal fluid) μ_{ex} through the following equation

$$\left(\frac{k}{k_S}\right) = 1 + \frac{\beta}{\phi}\int_0^{\phi} \phi' \frac{d\mu_{ex}(\phi_{HS}, \phi')}{d\phi'} d\phi' = Z(\phi) \tag{6}$$

where $Z(\phi)$ is the compressibility factor of the fluid, with ϕ being the packing fraction of particles in the fluid and $\beta = (k_B T)^{-1}$. The last passage follows from a standard thermodynamic relation between the excess chemical potential and the compressibility factor.[23] While eq 6 has been worked out for a monodisperse fluid, the argument leading to this result can be readily generalized to bimolecular encounters in a fluid mixture (Figure 8). In particular, we can repeat the derivation described in ref 23 and use a standard thermodynamic relation between the excess chemical potential and the compressibility factor of the hard sphere−collagen mixture $Z(\phi_{HS}, \phi_c)$, namely,

$$Z(\phi_{HS}, \phi_c) = 1 + \frac{\beta}{\phi_c}\int_0^{\phi_c} \phi' \frac{d\mu_{ex}(\phi_{HS}, \phi')}{d\phi'} d\phi' \tag{7}$$

which leads to the following intriguingly simple expression for the collagen−collagen encounter rate

$$\frac{k}{k_S} = Z(\phi_{HS}, \phi_c) \tag{8}$$

The increase in the encounter rate between two collagen monomers with respect to the ideal case equals the compressibility factor of the mixture. This result should be understood in the following way: the ideal case is $\phi_c \to 0$, while the packing fraction of the HS component enters the expression as a *parameter*. Moreover, we emphasize that no assumptions have been made as to the kind of molecules forming the binary mixture. The above formula is therefore appropriate for investigating bimolecular encounters in HS mixtures as well as mixtures of hard spheres and more complicated nonspherical objects. As a consequence, eq 8 may be employed to study how the measured nucleation and growth rates vary with increasing concentration of crowding agents. Toward this aim, it is convenient to study the *normalized* rate, i.e., the rate normalized to the value corresponding to the monodisperse collagen fluid ($\phi_{HS} = 0$),

$$\hat{k}(\phi_{HS}) \equiv \frac{k(\phi_{HS}, \phi_c)}{k(0, \phi_c)} = \frac{Z(\phi_{HS}, \phi_c)}{Z(0, \phi_c)} \tag{9}$$

Model 1: Nucleation in a Hard Spherocylinder-Hard Sphere (HSC-HS) Model. In the case of nucleation in the presence of Ficoll 400 crowders, Ficoll and collagen molecules are present in comparable molarities. Let us consider explicitly the case where crowding agents are nearly spherical Ficoll 400 molecules. A collagen monomer—a triple helix comprising three tightly wound alpha-chains—can be modeled as a long hard rod or hard spherocylinder (HSC) with a length of $L \approx 220 \pm 10$ nm and diameter of $\sigma \approx 4 \pm 1$ nm,[24] while Ficoll 400 molecules are well approximated by hard spheres of a hydrodynamic diameter $D \approx 20$ nm (as measured by dynamic light scattering of Ficoll 400 solutions in PBS, at room temperature). The formation of collagen aggregates can be interpreted in terms of a nematic-like ordering process, where the alignment of collagen monomers into fibrils is the consequence of large enthalpic interactions, namely, brought about by the potential energy associated with the polymerization of collagen monomers. An explicit expression for the compressibility of a HSC−HS mixture has been computed recently in the framework of the Parsons−Lee theory,[25] namely,

$$Z(\phi_{HS}, \phi_{HSC}) = 1 + \frac{[2 - (\phi_{HS} + \phi_{HSC})](Q\chi^2\phi_{HSC}^2 + P\chi\phi_{HS}\phi_{HSC} + 8\phi_{HS}^2)}{4(\phi_{HS} + \chi\phi_{HSC})[1 - (\phi_{HS} + \phi_{HSC})]^3} \tag{10}$$

where

$$\begin{cases} Q = \dfrac{3G[f]L^{*2} + 12L^* + 8}{D^{*3}} \\ P = \left(1 + \dfrac{1}{D^*}\right)^2\left(1 + \dfrac{1}{D^*} + \dfrac{3L^*}{2D^*}\right) \\ \chi = \dfrac{2D^{*3}}{3L^{*2} + 2} \end{cases} \tag{11}$$

with $L^* = L/\sigma$ and $D^* = D/\sigma$. The function $G[f] \in [0, 1]$ can be thought of as an order parameter for the nematic−isotropic phase transition. It depends on the probability density $f(\Omega)$ of the (solid) angle describing the orientation of sphero-cylinders with respect to the nematic axis, i.e.,

$$G[f] = \frac{4}{\pi}\int |\sin\psi(\Omega, \Omega')| f(\Omega) f(\Omega')\, d\Omega\, d\Omega' \tag{12}$$

where $\psi(\Omega, \Omega')$ is the angle formed by the axes of two HSCs identified by the two solid angles Ω and Ω' with respect to a fixed reference frame.

In the case of purely entropic nematic ordering, the parameter $G[f]$ is temperature-independent. We posit here that the same functional form for the HSC−HS mixture compressibility as given by eq 10 can be used in our case by making the parameter $G[f]$ temperature-dependent, thus accounting for the enthalpic interactions that drive the collagen assembly process. This can be done in a particularly simple way by resorting to the following analogy. The nematic-like ordering process underlying collagen polymerization can be thought of in terms of the alignment of an ensemble of permanent magnets in the presence of a magnetic field (paramagnetism). This implies the introduction of a polymerization enthalpy u_p, gauging the short-range potential energy that drives the stabilization of monomer−monomer encounter complexes. According to the above analogy, we can posit a temperature-dependent distribution of the direction of HSC axes, $f(\Omega, T)$,

$$f(\Omega, T) = \frac{1}{Z} e^{-\beta u_p \cos\theta} \tag{13}$$

where θ is the angle between the HSC axis (collagen monomers are chiral) and the nematic-like axis identified by the parallel stacking of collagen monomers and $\beta = 1/k_B T$. The normalization condition $\int f(\Omega, T)\, d\Omega = 1$ allows us to compute the constant Z (one-particle partition function). We obtain

$$f(\Omega, T) = \frac{\beta u_p}{4\pi \sinh(\beta u_p)} e^{-\beta u_p \cos\theta} \tag{14}$$

Inserting eq 14 into the definition (eq 12) and assuming as usual that the axis of one of the two HSCs coincides with the

DOI: 10.1021/jp5077559
J. Phys. Chem. B XXXX, XXX, XXX−XXX

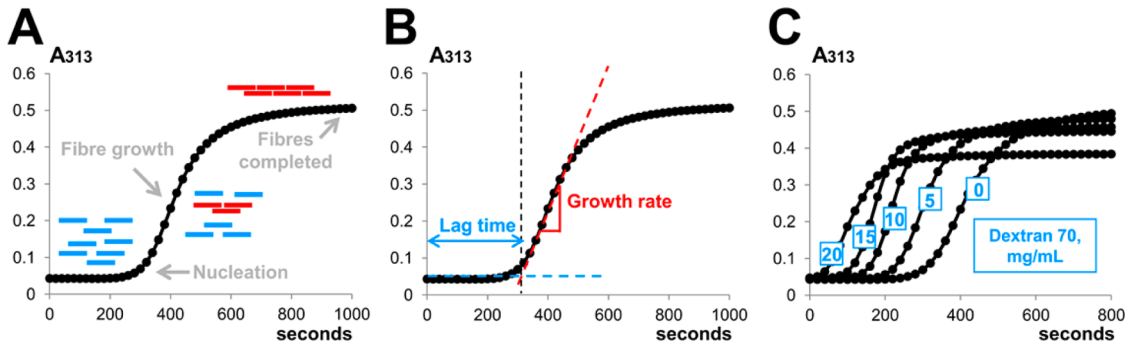

Figure 1. (A) Increase of turbidity in a sample containing aggregating collagen monomers *in vitro*. The initial lag phase is terminated by an increase in absorbance, the latter marking the end of nucleation time. A sigmoidal growth phase follows, during which nuclei are elongated into fibers by the lateral incorporation of freely diffusing monomers. (B) The growth rate can be defined as the slope in the quasi-linear section of the sigmoid, i.e., the slope at the inflection point. The intersection of the tangent with the baseline marks the nucleation time. (C) Different concentrations of the crowder dextran 70 kDa affect the course of turbidity over time, notably shortening the initial lag phase.

nematic-like axis, the integrals can be easily evaluated. This finally yields

$$G[T] = \frac{2I_1(\beta u_p)}{\sinh(\beta u_p)} \approx \begin{cases} 1 - \dfrac{(\beta u_p)^2}{24} & \text{for } \beta u_p \ll 1 \\ \sqrt{\dfrac{8}{\pi \beta u_p}} & \text{for } \beta u_p \gg 1 \end{cases} \quad (15)$$

where $I_1(x)$ is the modified Bessel function of the first kind of order one. In the isotropic phase at high temperatures ($\beta u_p \ll 1$), $G(T) \to 1$, while as the temperature decreases $G(T) \to 0$. We have found that a reasonable estimate of the enthalpy u_p associated with stabilization of monomer−monomer encounter complexes can be approximated to $u_p \approx 66.8$ kJ mol^{-1} (see Appendix I: nucleation activation energy calculation). This gives $G \in [0.263, 0.266]$ in the temperature range $T \in [28, 37]$ °C.

Model 2: Fiber Growth in a Hard Sphere (HS) Model. At the stage of fiber growth, a significant portion of collagen monomers have been incorporated into nuclei and nascent fibrils. Therefore, the population of collagen monomers has become significantly reduced relative to the population of Ficoll crowders. Therefore, fiber growth should be described by the ideal case $\phi_c \to 0$: the compressibility of the mixture tends to the HS compressibility, namely, $Z(\phi_{HS}, \phi_c) \to Z_{HS}(\phi_{HS})$, while $Z(0, \phi_c) \to 1$. In this limit (mathematically at order 0 in ϕ_c), eq 9 is simplified to

$$\hat{k}(\phi_{HS}) \approx Z_{HS}(\phi_{HS}) = \frac{1 + \phi_{HS} + \phi_{HS}^2 - \phi_{HS}^3}{(1 - \phi_{HS})^3} \quad (16)$$

where we have used the Carnahan−Starling expression for the HS compressibility.[26]

4. Void Volume Simulation *in Silico*. Using the Avogadro 1.1.0 software,[27] we generated a simplified immobile 3D system composed of "big crowders" (carbon-based pentahedra, with a width of 6.8 Å) and/or "small crowders" (carbon-based cube, with a width of 3.6 Å). The molecular coordinates were saved in a .pdb format for analysis. A 7 Å diameter spherical probe was then allowed to explore the vicinity of crowders with fixed locations in an unbounded 3D space (using an online tool published by Voss et al.[28]). Since the size of the exploring probe is limited to 10 Å by the online tool, pentahedra and cubes were suitable to materialize crowders with a size comparable to that of the probe. The total volume inaccessible to the spherical probe (Å^3) was calculated in different crowding conditions.

RESULTS

1. Ficoll Crowding Boosts the Kinetics of Collagen I Assembly *in Vitro*. Collagen I monomers *in vitro* first assemble into short bundles—the *nuclei*—which are subsequently elongated by the addition of freely diffusing monomers exploring their surface, to finally yield collagen fibers. In contrast to free monomers, collagen fibers diffract light due to their tubular nature. This diffraction is optimum for near UV wavelengths, and the wavelength of 313 nm was chosen to observe diffraction. This allows indirect spectrophotometric observation of *in vitro* fibrillogenesis—*turbidimetry* (Figure 1A).[19,29]

The two sequential phases of fibrillogenesis, nucleation and fiber growth, feature independent rates, which can be determined graphically (Figure 1B). The effects of six macromolecular crowders (PVP 40 kDa and 360 kDa, dextran 70 kDa and 200 kDa, and Ficoll 70 kDa and 400 kDa) on the kinetics of fibrillogenesis were assessed by turbidimetry. The crowder dextran 70 kDa, for instance, together with all the crowders tested, shortens the lag time and affects fiber growth proportionally to its concentration (Figure 1C).

The fiber growth rate was defined graphically as the slope of the linear section of the sigmoidal 313 nm absorbance curve, according to published methods.[19a] Accordingly, the nucleation time t_n was defined as the intersection between the baseline and the tangent to the sigmoidal section of the turbidity curve at the estimated inflection point (Figure 1B), according to established methods.[19a,30] From this, the nucleation rate was calculated as $k_n = 1/t_n$. We first focused on the spherical crowder Ficoll 400, with which we tested the effect of crowding on the rates of collagen nucleation k_n and of fiber growth k_a (Figure 2).

Nucleation and elongation feature comparable rates at a given temperature in uncrowded conditions (0 mg·mL^{-1} Ficoll 400), and both reactions proceed faster upon increasing the temperatures (Figure 2). Crowding is seen to boost both reactions. However, the nucleation process appears to be more accelerated by macromolecular crowding (MMC) with respect to fiber elongation.

2. The Entropic Contribution of Crowding to Fibrillogenesis. The experimental evidence is that crowding enhances both nucleation and fiber growth (elongation) rates, which are seen to increase with increasing concentration of crowding

DOI: 10.1021/jp5077559
J. Phys. Chem. B XXXX, XXX, XXX−XXX

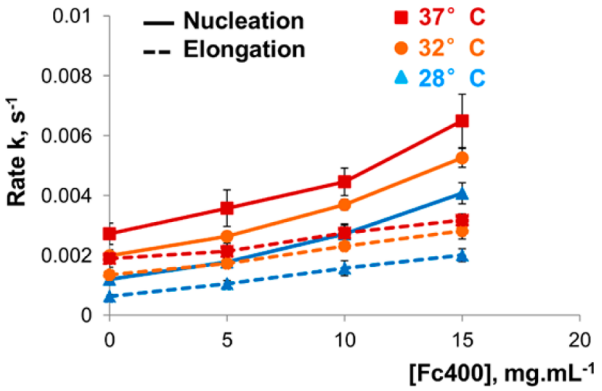

Figure 2. Fiber growth rate (k_a) and inverse lag time (k_n) as functions of temperature and crowding concentration. Error bars represent the standard deviation, $n = 4$.

agents in the tested range [0−20] mg·mL^{-1}. We lay down theoretical arguments to explain this remarkable experimental evidence as follows.

Nucleation in a Hard Spherocylinder-Hard Sphere (HSC-HS) Model. We developed a mathematical model which yields the theoretical relative nucleation rates in the presence of crowders (see the Materials and Methods). This nucleation model considers that crowding effects are purely entropic, and takes into account the known enthalpic interactions between collagen monomers. A comparison between theoretical and experimental nucleation data can therefore infirm or confirm the hypothesis that crowding effects on nucleation are purely entropic (Figure 3). The theoretical expression for the

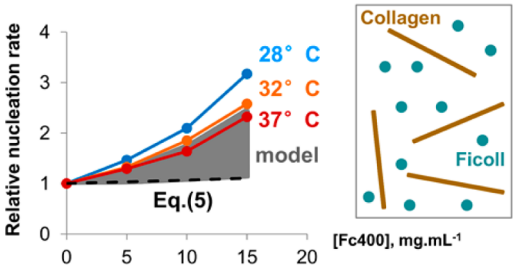

Figure 3. Experimental values of the relative nucleation rates k/k_0 compared with the HSC-HS model (gray range). The system can be described as a mixture of spherical Ficoll crowders with spherocylindrical collagen monomers in comparable molarities. Rates were measured at different temperatures and crowder concentrations. Experimental data are better described by the purely entropic model as temperature is raised from 28 °C (blue) to 32 °C (orange) and 37 °C (red). The estimation of relative rates by a purely EVE-based effective-medium argument (eq 5) is displayed for comparison (black dashed line).

normalized rate eq 8 (combined with eqs 10 and 15) turns out to be rather sensitive to changes in the structural parameters of collagen monomers. The dimensions of hydrated collagen monomers were determined experimentally by Bernengo et al., and feature standard deviations so that $L \approx 220 \pm 10$ nm and $\sigma \approx 4 \pm 1$ nm.[24] As a result, the theoretical rate of nucleation is given by a range reflecting the choice of possible values for L and σ (Figure 3, gray area). We observed that relative increases in nucleation rates are less pronounced at higher temperatures (37 °C versus 28 °C). The 32 and 37 °C curves overlap the theoretical range (gray area) but do not compare with the relative nucleation rates yielded by eq 4 (simple EVE effective-medium estimation; see the Materials and Methods).

Fiber Growth in a Hard Sphere (HS) Model. By analogy to nucleation, a specific entropic model was designed to describe relative elongation rates in crowded environments. This model takes into consideration the fact that a number of collagen monomers have been incorporated into fibers, and that their concentration is significantly reduced with respect to the concentration of crowders (see the Materials and Methods). We employed eq 16 to predict the relative constant rates of collagen elongation, and compared our predictions with experimental measurements between 28 and 37 °C (Figure 4).

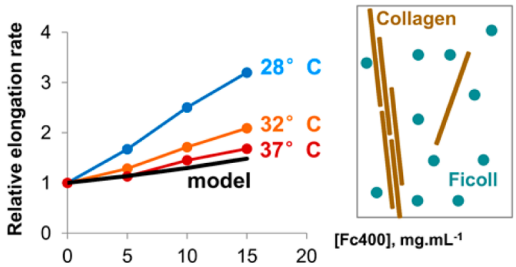

Figure 4. Theoretical (black) and experimental rates of fiber growth measured at 28 °C (blue), 32 °C (orange), and 37 °C (red). The proportion of free collagen monomers is negligible compared to that of Ficoll particles, so that the collagen monomer-crowding agent mixture can be modeled as a homogeneous solution of hard spheres. The data fit the model at higher temperature, possibly due to a relative decrease in enthalpic interactions.

The effect of macromolecular crowding on the relative elongation rates is of lower intensity at higher temperatures. In addition, the 37 °C experimental data match the theoretical curve calculated solely on the basis of entropic considerations. It is unclear why the relative increase in the rates is more pronounced at lower temperatures. This probably reflects a higher relative contribution of enthalpic terms to the driving forces of the self-assembly process.

3. Long-Range Synergistic Effects in Mixtures of Crowders. First, we sought to investigate *in silico* the volume occupancy generated by big and small crowders in the vicinity of each other. We simulated three different immobile spatial configurations, using big (6.8 Å) and/or small (3.6 Å) crowders. A 7 Å spherical probe was then used to explore the accessible volume of the system, in analogy to the van der Waals surface, using an approach designed by Voss and Gerstein[28] (Figure 5).

Molecular simulations show that the volume excluded in a mixture of crowders is significantly higher than the added volumes of single-species crowding agents, as the probe is excluded from an extra narrow space between crowders (Figure 5). This narrow space, in this simple simulation, creates an extra 26% of volume exclusion.

Second, we designed an *in vitro* experiment to assess the crowding power of mixtures of big and small crowders: the speed of collagen nucleation was monitored in the presence of big (Ficoll 400, dextran 200, or PVP 360) and/or small (Ficoll 70, dextran 70, or PVP 40) crowders (Figure 3). We tested a *null hypothesis* (NH), namely, that crowding effects in a mixture are purely additive (we refer to the NH as *theory* in the following). On the basis of this hypothesis, we calculated

DOI: 10.1021/jp5077559
J. Phys. Chem. B XXXX, XXX, XXX−XXX

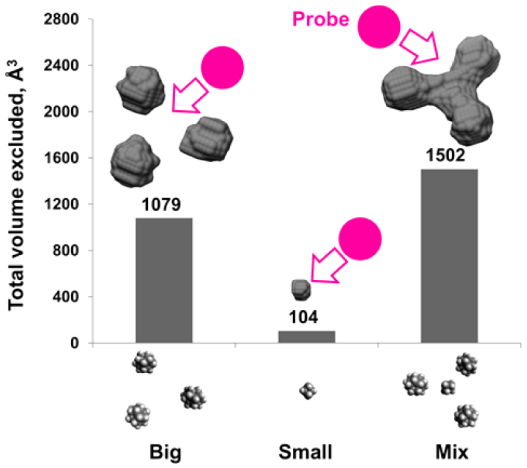

Figure 5. Total volume excluded by 3 big and/or 1 small crowder(s) in homo- or heterocrowding conditions. In the "mix" condition, the small crowder does not occupy a significant volume but reduces the average distance between crowders to a value lower than the probe diameter: a void volume is created. The total excluded volume is therefore greater than the sum of the crowders' volumes, as the small crowder is granted with extra volume occupancy (the void volume) due to its proximity to the big crowders.

theoretical effects of mixed crowding in a mixture by adding the effects of each population measured separately (see the Materials and Methods). We finally compared theoretical and experimental effects of mixed crowding at 37 °C (Figure 6). We observed that experimental lag times are consistently shorter than those calculated by neglecting the extra void volume effect, for all mixtures tested. The observed differences are statistically significant for the mixtures of PVP and Ficoll.

The gap between experimental and theoretical lag times can reach 20% of theoretical data (5:5 PVP mix, Figure 6). The amount of crowders is an important factor, as the significant gap between experimental and theoretical data in a (5:5) Ficoll mix is absent in a (10:10) Ficoll mix. Trends in dextran mixtures also suggest an important role of the mixing ratio, as gaps range from (10:5) to (5:5) mixtures (9 and 16%, respectively).

DISCUSSION

Effects of Crowding on Fibrillogenesis. The volume occupancy of crowders is known to reduce the space available to freely diffusing collagen monomers, raising their effective concentration. An increasing concentration of Ficoll 400 between 0 and 15 mg·mL^{-1} thus drives collagen nucleation and fiber growth, similarly to a rise in collagen concentration.[19a] In the case of diffusion-limited aggregations such as collagen assembly, reaction rates are a direct function of reactant encounter rates, themselves being functions of reactant size. It is thus understandable that monomer−monomer encounter (leading to nucleation) is less likely than fiber−monomer encounter (elongation), and that nucleation is therefore accelerated by crowding to a greater extent than elongation (Figure 2). Importantly, the concentration of crowders in this study is maintained low (up to 20 mg·mL^{-1}) to avoid high-concentration-related detrimental effects—such as confinement and viscosity—on collagen diffusion rates.

Entropic Origin of Crowding Effects. We developed models of crowding effects, assuming purely entropic interactions among crowders and between crowders and collagen monomers. For both nucleation and elongation, our models (eqs 10 and 15) describe accurately the experimental data at 37 °C; this suggests that the effects of Ficoll crowding on collagen fibrillogenesis are of entropic origin, i.e., essentially volume exclusion due to a competition for access to space. The gap between experimental data and the models which is observed at lower temperatures might signal the appearance of enthalpic interactions, in line with an earlier report of the appearance of enthalpic (soft-core) interactions as temperature decreases in crowded systems.[31] Importantly, in the case of nucleation, the simple effective-medium argument to account for excluded-volume boosting of diffusive encounters leading to eq 5 largely underestimates the experimental measurements (see dashed line in Figure 3), showing that physical arguments from the theory of nonideal solutions are needed to capture the experiments. We can conclude that, at physiological temperatures, Ficoll crowders essentially boost nucleation and fiber growth by volume exclusion (EVE). It is interesting to note the crowder's size has no significant effect on nucleation kinetics (Figure 3), whereas it is known to affect reaction equilibria.[9a] Additionally, we calculated that additional entropic effects of crowders, such as depletion forces, are only likely to be at work between large collagen aggregates and high crowder concentration (see Appendix II), thus boosting the more advanced stages of the aggregation process after the fiber elongation stage. Moreover, we show that the depth of the depletion attractive potential arising in the gap between two collagen monomers due to the volume excluded to crowders is at most

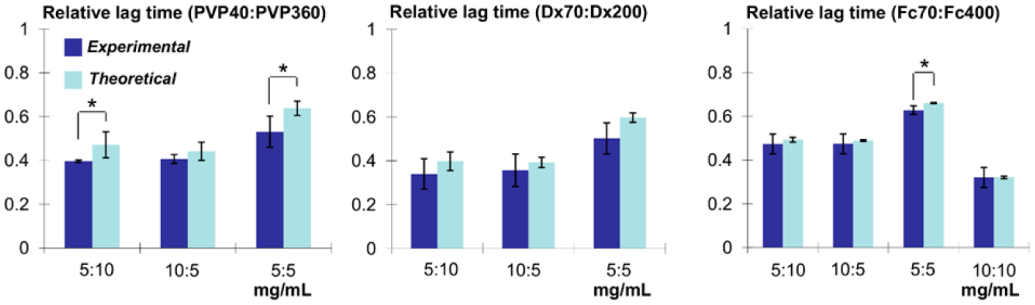

Figure 6. Experimental and theoretical relative lag times in heterogeneous mixtures of crowders. Three mixtures of crowders were tested: (PVP 40:PVP 360), (dextran 70:dextran 200), (Ficoll 70:Ficoll 400). Experimental lag times are consistently smaller than their theoretical (NH) counterparts, suggesting that the hypothesis of purely additive crowding effects in a mixture underestimates the efficiency of mixed crowding. Statistically significant differences between theoretical and experimental lag times are represented as * ($P > 0.95$). Error bars represent standard deviations, $n = 4$.

DOI: 10.1021/jp5077559
J. Phys. Chem. B XXXX, XXX, XXX−XXX

5% (Ficoll 70)/30% (Ficoll 400) of the enthalpy of polymerization (Appendix I) at the largest crowding concentrations considered (see Appendix II).

Void Volumes Create Long-Range Crowding Effects. The principle of volume exclusion can be illustrated by a still picture of a system hosting crowders and a like-sized test particle. In some cases, the interspace between two crowders is too narrow to accommodate a test particle: as a result, the test particle is not only excluded from the space occupied by crowders but also from these narrow interspaces which sum up to create a *void volume*. The volume occupied by crowders is then combined to the void volume—depicted in light blue in Figure 7, left panel—to make up the total excluded volume. In single-species crowding conditions, the void volume is proportional to the concentration of crowders.

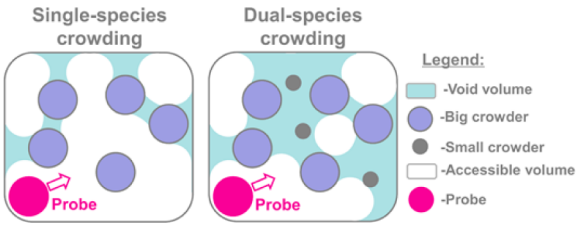

Figure 7. Volume exclusion in single-species (left) and dual-species (right) crowding conditions. The void volume between crowders is inaccessible to a like-sized probe, by analogy to a van der Waals surface. This void volume provides small crowders with extra volume-excluding efficiency (with respect to their true excluded volume) when in the vicinity of big crowders, generating a synergic effect in dual-species crowding conditions.

It is therefore expected that the total excluded volume increases linearly with crowder concentration. However, we observe that a high percentage of the accessible space between crowders can be made unavailable to the test particle by the addition of a few smaller crowders (Figure 7, right panel). In such a case, the small crowders occupy a negligible volume but significantly increase the total void volume by reducing the average distance between crowders, in a *gating* fashion. The total volume of crowders increases only slightly, but the void volume—hence the total excluded volume—increases significantly. Summarizing, small crowders create more total excluded volume in the vicinity of big crowders than in the bulk. We suggest that this *gating* principle, which influences kinetic parameters, is the basis of synergistic effects observed by previous research groups in mixed-crowding conditions.[16] Most importantly, this mechanism seems to dominate at physiological temperature (37 °C), while other effects set in at lower temperatures. It is interesting to observe that this is consistent with recent theoretical results by Shah and colleagues, who suggested that enthalpic effects prevail in mixtures at lower temperatures (27 °C).[17]

The notion of gating is illustrated by our computer simulations, which suggest the existence of a void volume between neighboring big and small crowders. Within the example of conformation we chose to simulate, we measured that 26% of the total excluded volume results from the void volume. The existence of a void volume in mixed crowding conditions was further ascertained by *in vitro* experiments. We summed the effects of Ficoll 400 and Ficoll 70 alone on the relative nucleation lag times at 37 °C, and compared our results with experimental measurements using the corresponding mixing ratios. We repeated the process with dextran 200/dextran 70 and PVP 360/PVP 40. We discovered that our calculation method underestimated the measured lag times in most cases, with a gap of up to 20%. We suggest that this underestimation originates from the neglect of void volumes in our calculation method. This hypothesis is supported by our previous conclusions on the purely entropic nature of crowding effects at 37 °C. Finally, *in silico* and *in vitro* measurements of the sole void volume yield comparable values (26 and 20%, respectively), further supporting our conclusion. Importantly, the crowding effect of the void volume is not only detected for near-spherical crowders (Ficoll) but also for linear crowders (PVP), which adopt random, nonspherical conformations in solution. Our conclusions can thus be extrapolated to all crowding conditions, regardless of the crowders' shape.

CONCLUSION

We demonstrated how crowding efficiencies on kinetic parameters can be significantly boosted by means of mixing heterogeneous populations of crowders. Moreover, we showed how simple concepts from the theory of nonideal solutions can be employed to rationalize the experiments. Indeed, crowders do not need to occupy a volume to exclude it: a long-range synergistic effect is possible in mixtures, providing small crowders with extra volume occupancy when in the vicinity of bigger crowders, in analogy to a van der Waals surface. It would also be important to test such synergistic effects on simpler biochemical reactions with a better characterized activation energy. Mixed crowding is possibly a feature allowing nature to create more EVE with less crowders; further *in vitro* enhancements of crowding power, from dual to multiple populations like blood serum, could be achieved with a similar nature-mimicking approach.

APPENDIX I

Calculation of the Nucleation Activation Energy. The enthalpy of collagen assembly u_p can be determined via a temperature scan. Indeed, the constant rate of nucleation obeys the Arrhenius law (eq 17)

$$k_n = k_{n,\infty} e^{-(u_p/RT)} \tag{17}$$

where R is the gas constant and T is the temperature (K). The plot $\ln(k) = f(1/T)$ in the interval [28 °C; 37 °C] features a slope $(-u_p/R)$, from which the value of u_p was calculated (Figure 8).

APPENDIX II

Critical Length of Collagen Fibrils for Ficoll-Mediated Depletion Interactions. The depletion interaction potential arising in a fluid of spherical objects of diameter σ between two parallel cylinders of length L and radius r whose surfaces lie at distance d can be calculated according to Krüger et al.:[32]

$$\frac{u_d(d)}{k_B T} = \begin{cases} \frac{4L\sqrt{r}}{3}(\sigma - d)^{3/2}\rho Z(\Phi) & \text{for } d < \sigma \\ 0 & \text{for } d > \sigma \end{cases} \tag{18}$$

where ρ is the number density of the fluid of spherical molecules and $Z(\Phi)$ its compressibility. In the hypothesis that these molecules behave as hard spheres, one can safely use the Carnahan−Starling expression

DOI: 10.1021/jp5077559
J. Phys. Chem. B XXXX, XXX, XXX−XXX

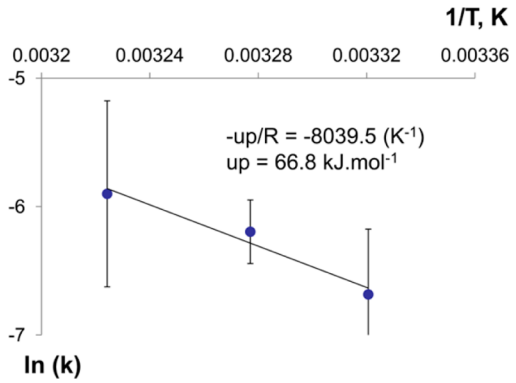

Figure 8. Arrhenius plot of logarithms of constant nucleation rates as a function of $(1/T)$. The linearity of the plot allows for the calculation of its slope, u_p/R, from which we extracted the approximate enthalpy of collagen assembly u_p = 66.8 kJ mol^{-1}. Error bars represent standard deviations, n = 4.

$$Z(\Phi) = \frac{1 + \Phi + \Phi^2 - \Phi^3}{(1 - \Phi)^3} \tag{19}$$

Collagen monomers are characterized by short-range interactions between them, whose enthalpy we have estimated at $u_p \approx 66.8$ kJ mol^{-1}. We can thus compute the critical length L^* of a forming collagen fibril such that the depletion attraction arising from the exclusion of crowder molecules between two fibrils equals the collagen−collagen interaction. This value of L will provide an estimate of the critical length above which it is more advantageous in the system to start forming fibril bundles than to elongate existing fibrils through the addition of more collagen monomers. The critical length L^* corresponding to a fibril−fibril distance of half a crowder diameter, $d = \sigma/2$, is defined by the following condition

$$u_d(\sigma/2)|_{L=L^*} = u_p \tag{20}$$

which gives

$$L^* = \frac{3}{\sqrt{2}}\left(\frac{u_p}{k_B T}\right)\frac{1}{\rho Z(\Phi)\sigma\sqrt{r\sigma}} \tag{21}$$

The results of this calculation are plotted in Figure 9. The parameters used are listed in Table 1 following Fissell et al.[33] It is clear that at the lower concentrations rather long fibrils are formed through the addition of monomers, until these start interacting between them through depletion forces. However, at concentrations of the order of 15 mg·mL^{-1}, depletion forces set in much earlier, i.e., for shorter fibrils of the order of a few collagen monomers in length and diameter.

Table 1. Parameters Used in the Calculation

	Ficoll 70	Ficoll 400
molecular mass (kg mol^{-1})	39	93
diameter (nm)	11	20

Conversely, eq 18 can be used to compute the ratio between depletion energy and collagen−collagen polymerization enthalpy (Appendix I). Considering collagen monomers as cylinders of length 220 nm and diameter 4 nm a distance of a crowding agent radius apart, we obtain for a crowder concentration of 15 mg·mL^{-1}

$$\frac{u_d(\sigma/2)}{u_p} = \begin{cases} 0.05 \text{ (Ficoll 70)} \\ 0.33 \text{ (Ficoll 400)} \end{cases} \tag{22}$$

■ ASSOCIATED CONTENT

Supporting Information

Figures showing a schematic representation of a binary hard-spheres mixture comprising two species of diameter D and σ and the equivalent Smoluchowski representation of a binary encounter between S2 spheres (Figure S1), relative lag time as a function of Ficoll 400 concentration at a temperature of 37 °C (Figure S2), and relative lag time and growth rate as a function of crowder concentration (Figure S3). This material is available free of charge via the Internet at http://pubs.acs.org.

■ AUTHOR INFORMATION

Notes

The authors declare no competing financial interest.

■ ACKNOWLEDGMENTS

J.-Y.D. is a recipient of a scholarship from the NUS School of Integrative Sciences and Engineering (NGS). M.R. is grateful for the support from the NUS Tissue Engineering Programme, a Life Science Institute Programme.

■ REFERENCES

(1) Lareu, R. R.; Harve, K. S.; Raghunath, M. Emulating a Crowded Intracellular Environment in vitro Dramatically Improves RT-PCR Performance. *Biochem. Biophys. Res. Commun.* **2007**, *363* (1), 171−177.

(2) Zimmerman, S. B.; Minton, A. P. Macromolecular Crowding: Biochemical, Biophysical, and Physiological Consequences. *Annu. Rev. Biophys. Biomol. Struct.* **1993**, *22*, 27−65.

(3) Hong, J.; Gierasch, L. M. Macromolecular Crowding Remodels the Energy Landscape of a Protein by Favoring a More Compact Unfolded State. *J. Am. Chem. Soc.* **2010**, *132* (30), 10445−10452.

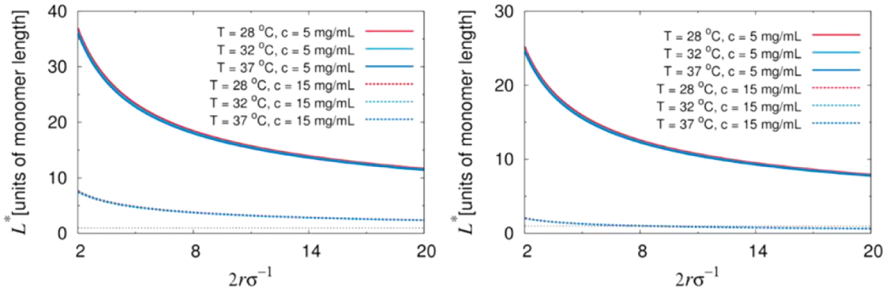

Figure 9. Critical length of collagen fibrils defined by eq 21 (units of the length of a single collagen monomer $L \approx 220$ nm) versus radius of the fibril (units of the diameter of collagen monomers $\sigma \approx 4$ nm) for Ficoll 70 (left panel) and Ficoll 400 (right panel)/collagen mixtures.

DOI: 10.1021/jp5077559
J. Phys. Chem. B XXXX, XXX, XXX−XXX

(4) (a) Dix, J. A.; Verkman, A. S. Crowding Effects on Diffusion in Solutions and Cells. *Annu. Rev. Biophys.* **2008**, *37*, 247−263. (b) Klumpp, S.; Scott, M.; Pedersen, S.; Hwa, T. Molecular Crowding Limits Translation and Cell Growth. *Proc. Natl. Acad. Sci. U.S.A.* **2013**, *110* (42), 16754−16759.

(5) Akabayov, B.; Akabayov, S. R.; Lee, S. J.; Wagner, G.; Richardson, C. C. Impact of Macromolecular Crowding on DNA Replication. *Nat. Commun.* **2013**, *4*, No. 1615.

(6) Tan, C.; Saurabh, S.; Bruchez, M. P.; Schwartz, R.; Leduc, P. Molecular Crowding Shapes Gene Expression in Synthetic Cellular Nanosystems. *Nat. Nanotechnol.* **2013**, *8* (8), 602−608.

(7) Zhang, C.; Shao, P. G.; van Kan, J. A.; van der Maarel, J. R. Macromolecular Crowding Induced Elongation and Compaction of Single DNA Molecules Confined in a Nanochannel. *Proc. Natl. Acad. Sci. U.S.A.* **2009**, *106* (39), 16651−16656.

(8) Forterre, P.; Mirambeau, G.; Jaxel, C.; Nadal, M.; Duguet, M. High Positive Supercoiling in vitro Catalyzed by an ATP and Polyethylene Glycol-Stimulated Topoisomerase from Sulfolobus acidocaldarius. *EMBO J.* **1985**, *4* (8), 2123−2128.

(9) (a) Chebotareva, N. A.; Kurganov, B. I.; Livanova, N. B. Biochemical Effects of Molecular Crowding. *Biochemistry (Moscow)* **2004**, *69* (11), 1239−1251. (b) Jiang, M.; Guo, Z. Effects of Macromolecular Crowding on the Intrinsic Catalytic Efficiency and Structure of Enterobactin-Specific Isochorismate Synthase. *J. Am. Chem. Soc.* **2007**, *129* (4), 730−731.

(10) Munishkina, L. A.; Cooper, E. M.; Uversky, V. N.; Fink, A. L. The Effect of Macromolecular Crowding on Protein Aggregation and Amyloid Fibril Formation. *J. Mol. Recognit.* **2004**, *17* (5), 456−464.

(11) (a) Cheung, M. S.; Klimov, D.; Thirumalai, D. Molecular Crowding Enhances Native State Stability and Refolding Rates of Globular Proteins. *Proc. Natl. Acad. Sci. U.S.A.* **2005**, *102* (13), 4753−4758. (b) Homouz, D.; Perham, M.; Samiotakis, A.; Cheung, M. S.; Wittung-Stafshede, P. Crowded, Cell-Like Environment Induces Shape Changes in Aspherical Protein. *Proc. Natl. Acad. Sci. U.S.A.* **2008**, *105* (33), 11754−11759. (c) Samiotakis, A.; Wittung-Stafshede, P.; Cheung, M. S. Folding, Stability and Shape of Proteins in Crowded Environments: Experimental and Computational Approaches. *Int. J. Mol. Sci.* **2009**, *10* (2), 572−588.

(12) Tellam, R. L.; Sculley, M. J.; Nichol, L. W.; Wills, P. R. The Influence of Poly(ethylene glycol) 6000 on the Properties of Skeletal-Muscle Actin. *Biochem. J.* **1983**, *213* (3), 651−659.

(13) Chen, C.; Loe, F.; Blocki, A.; Peng, Y.; Raghunath, M. Applying Macromolecular Crowding to Enhance Extracellular Matrix Deposition and its Remodeling In Vitro for Tissue Engineering and Cell-based Therapies. *Adv. Drug Delivery Rev.* **2011**, *63* (4−5), 277−290.

(14) Minton, A. P. The influence of Macromolecular Crowding and Macromolecular Confinement on Biochemical Reactions in Physiological Media. *J. Biol. Chem.* **2001**, *276* (14), 10577−10580.

(15) (a) Asakura, S.; Oosawa, F. Interaction Between Particles Suspended in Solutions of Macromolecules. *J. Polym. Sci.* **1958**, *33* (126), 183−192. (b) Marenduzzo, D.; Finan, K.; Cook, P. R. The Depletion Attraction: an Underappreciated Force Driving Cellular Organization. *J. Cell Biol.* **2006**, *175* (5), 681−686. (c) Tuinier, R.; Dhont, J. K. G.; Fan, T. H. How Depletion Affects Sphere Motion Through Solutions Containing Macromolecules. *Europhys. Lett.* **2006**, *75* (6), 929−935.

(16) (a) Zhou, H. X. Effect of Mixed Macromolecular Crowding Agents on Protein Folding. *Proteins* **2008**, *72* (4), 1109−1113. (b) Du, F.; Zhou, Z.; Mo, Z. Y.; Shi, J. Z.; Chen, J.; Liang, Y. Mixed Macromolecular Crowding Accelerates the Refolding of Rabbit Muscle Creatine Kinase: Implications for Protein Folding in Physiological Environments. *J. Mol. Biol.* **2006**, *364* (3), 469−482. (c) Batra, J.; Xu, K.; Zhou, H. X. Nonadditive Effects of Mixed Crowding on Protein Stability. *Proteins* **2009**, *77* (1), 133−138.

(17) Shah, D.; Tan, A. L.; Ramakrishnan, V.; Jiang, J.; Rajagopalan, R. Effects of Polydisperse Crowders on Aggregation Reactions: A Molecular Thermodynamic Analysis. *J. Chem. Phys.* **2011**, *134* (6), No. 064704.

(18) Parkinson, J.; Kadler, K. E.; Brass, A. Simple Physical Model of Collagen Fibrillogenesis Based on Diffusion Limited Aggregation. *J. Mol. Biol.* **1995**, *247* (4), 823−831.

(19) (a) Silver, F. H.; Birk, D. E. Kinetic Analysis of Collagen Fibrillogenesis: I. Use of Turbidity−Time Data. *Collagen Relat. Res.* **1983**, *3* (5), 393−405. (b) Farber, S.; Garg, A. K.; Birk, D. E.; Silver, F. H. Collagen Fibrillogenesis In Vitro: Evidence for Pre-nucleation and Nucleation Steps. *Int. J. Biol. Macromol.* **1986**, *8* (1), 37−42.

(20) Charlton, L. M.; Barnes, C. O.; Li, C.; Orans, J.; Young, G. B.; Pielak, G. J. Residue-Level Interrogation of Macromolecular Crowding Effects on Protein Stability. *J. Am. Chem. Soc.* **2008**, *130* (21), 6826−6830.

(21) Smoluchowski, M. V. Drei Vortrage uber Diffusion, Brownsche Bewegung und Koagulation von Kolloidteilchen. *Phys. Z.* **1916**, *17*, 27.

(22) Dorsaz, N.; De Michele, C.; Piazza, F.; De Los Rios, P.; Foffi, G. Diffusion-limited Reactions in Crowded Environments. *Phys. Rev. Lett.* **2010**, *105* (12), 120601.

(23) Piazza, F.; Dorsaz, N.; De Michele, C.; De Los Rios, P.; Foffi, G. Diffusion-limited Reactions in Crowded Environments: a Local Density Approximation. *J. Phys.: Condens. Matter* **2013**, *25* (37), 375104.

(24) Bernengo, J. C.; Ronziere, M. C.; Bezot, P.; Bezot, C.; Herbage, D.; Veis, A. A Hydrodynamic Study of Collagen Fibrillogenesis by Electric Birefringence and Quasielastic Light Scattering. *J. Biol. Chem.* **1983**, *258* (2), 1001−1006.

(25) Cuetos, A.; Martinez-Haya, B.; Lago, S.; Rull, L. F. Use of Parsons-Lee and Onsager Theories to Predict Nematic and Demixing Behavior in Binary Mixtures of Hard Rods and Hard Spheres. *Phys. Rev. E: Stat., Nonlinear, Soft Matter Phys.* **2007**, *75* (6 Pt 1), 061701.

(26) Carnahan, N. F.; Starling, K. E. Equation of State for Nonattracting Rigid Spheres. *J. Chem. Phys.* **1969**, *51* (2), 635−636.

(27) Hanwell, M. D.; Curtis, D. E.; Lonie, D. C.; Vandermeerschd, T.; Zurek, E.; Hutchison, G. R. Avogadro: An Advanced Semantic Chemical Editor, Visualization, and Analysis Platform. *J. Cheminf.* **2012**, *4* (8).

(28) Voss, N. R.; Gerstein, M. 3V: Cavity, Channel and Cleft Volume Calculator and Extractor. *Nucleic Acids Res.* **2010**, *38* (Web Server issue), W555−W562.

(29) Morris, A. M.; Watzky, M. A.; Finke, R. G. Protein Aggregation Kinetics, Mechanism, and Curve-Fitting: a Review of the Literature. *Biochim. Biophys. Acta* **2009**, *1794* (3), 375−397.

(30) (a) Tsai, S. W.; Liu, R. L.; Hsu, F. Y.; Chen, C. C. A Study of the Influence of Polysaccharides on Collagen Self-Assembly: Nanostructure and Kinetics. *Biopolymers* **2006**, *83* (4), 381−388. (b) Na, G. C.; Butz, L. J.; Carroll, R. J. Mechanism of In Vitro Collagen Fibril Assembly. Kinetic and Morphological Studies. *J. Biol. Chem.* **1986**, *261* (26), 12290−12299.

(31) Zhou, H.-X. Polymer Crowders and Protein Crowders Act Similarly on Protein Folding Stability. *FEBS Lett.* **2013**, *587* (5), 394−397.

(32) Krüger, S.; Mögel, H. J.; Wahab, M.; Schiller, P. Depletion Force Between Anisometric Colloidal Particles. *Langmuir* **2011**, *27* (2), 646−650.

(33) Fissell, W. H.; Hofmann, C. L.; Smith, R.; Chen, M. H. Size and Conformation of Ficoll as Determined by Size-exclusion Chromatography Followed by Multiangle Light Scattering. *Am. J. Physiol. Renal Physiol.* **2010**, *298* (1), F205−F208.

DOI: 10.1021/jp5077559
J. Phys. Chem. B XXXX, XXX, XXX−XXX